

Reflected image of a strongly focused spot

Lukas Novotny

The Institute of Optics, University of Rochester, Rochester, New York 14627

Robert D. Grober

Department of Applied Physics, Yale University, New Haven, Connecticut 06520

Khaled Karrai

Center for NanoScience, Sektion Physik der Ludwig Maximilian University, Geschwister-Scholl-Platz 1, 80539, Munich, Germany

Received December 19, 2001

We describe the reflection of a strongly focused beam from an interface between two dielectric media. If the beam is incident from the optically denser medium, the image generated by the reflected light is strongly aberrated. This situation is encountered in high-resolution confocal microscopy and data sampling based on solid immersion lenses and oil immersion objectives. The origin of the observed aberrations lies in the nature of total internal reflection, for which there is a phase shift between incident and reflected waves. This phase shift displaces the apparent reflection point beyond the interface, similarly to the Goos–Hänchen shift.

© 2001 Optical Society of America

OCIS codes: 110.0110, 120.0120, 180.0180, 210.0210, 240.0240, 260.0260.

In various experimental situations light is focused on or near an interface between dielectric media. For some techniques such as confocal microscopy and laser tweezers the focused light is incident from the optically denser medium. If the numerical aperture (NA) of the focusing lens is sufficiently large, some field components of the focused light undergo total internal reflection (TIR) at the interface. Under these conditions the reflected wave is phase shifted with respect to the incident wave and the apparent reflection point appears to be displaced beyond the interface.

In this Letter we theoretically describe the reflected image of a laser beam focused near a glass–air interface. It is found that the reflected image appears strongly aberrated if the focused light possesses field components that are totally internally reflected at the interface. The significance of this aberration in the context of reflection-type confocal microscopy with solid immersion lenses was recently analyzed.¹ The aberrations were predicted in 1952 by Maeckler and Lehmann,² who analyzed the reflected field of a point source near a dielectric interface by using both a geometrical optics and a scalar wave theory approach. Shortly after, the aberrations were experimentally verified by Lehmann and Maeckler.³ Here we present a rigorous but physically intuitive derivation based on the angular spectrum representation of optical fields.

Our analysis is based on the configuration shown in Fig. 1. A 45° beam splitter reflects part of the incoming beam upward, where it is focused near a planar interface by a high-NA objective lens. The distance between focus ($z = 0$) and interface is designated z_0 . The reflected field is collected by the same lens, transmitted through the beam splitter, and then focused by a second lens onto the image plane. Whereas the fields near the interface were recently investigated,^{4,5} we intend to derive the field distribution in the image plane. We assume that both lenses are aplanatic to fulfill the sine condition and the power law of geometrical optics.

To start, we remove the medium with index n_2 and consider a homogeneous medium with index n_1 . We choose a coordinate system at the geometrical focus of the high-NA lens (f) and express the electric field \mathbf{E} near the focus in terms of an angular spectrum as

$$\mathbf{E}(r) = \frac{1}{2\pi} \iint_{k_x, k_y} \hat{\mathbf{E}}(k_x, k_y) \exp(i\mathbf{k} \cdot \mathbf{r}) dk_x dk_y. \quad (1)$$

Here k_x and k_y denote the transverse components of wave vector \mathbf{k}_1 ($k_1 = n_1 2\pi/\lambda$) and $k_{z_1} = [k_1^2 - (k_x^2 + k_y^2)]^{1/2}$ is the corresponding longitudinal wave number. The integration runs over the range of spatial frequencies defined by the NA of the focusing lens. $\hat{\mathbf{E}}$ denotes the Fourier spectrum of the electric field

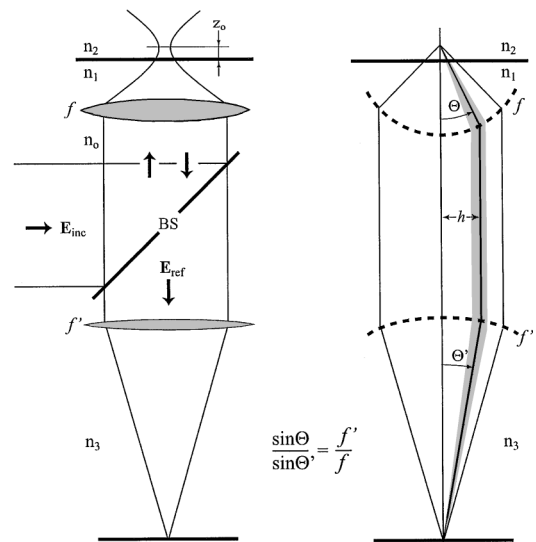


Fig. 1. A linearly polarized beam is reflected by a beam splitter (BS) and focused by a high-NA objective lens with focal radius f onto an interface between two dielectric media, n_1 and n_2 . The reflected field is collected by the same lens, transmitted through the beam splitter, and refocused by a second lens with focal radius f' onto the image plane.

evaluated at $z = 0$. It can be expressed in terms of the far field \mathbf{E}_∞ on reference sphere f as⁶

$$\hat{\mathbf{E}}(k_x, k_y) = \frac{if \exp(-ik_1 r)}{k_{z_1}} \mathbf{E}_\infty(k_x, k_y, k_{z_1}), \quad (2)$$

where the far field \mathbf{E}_∞ is evaluated in the direction of the dimensionless unit vector $\hat{s} = (k_x/k_1, k_y/k_1, k_{z_1}/k_1) = (x/f, y/f, z/f)$.

We assume that the incident field $\mathbf{E}_{\text{inc}} = E_o \hat{n}_x$ is a weakly focused Gaussian beam polarized along the x direction and with a beam waist much larger than the extent of the focusing lens (overfilled back aperture). After being refracted at reference sphere f , the incident field corresponds to \mathbf{E}_∞ , and the field near the focus can be evaluated from Eq. (1).⁷ Next we introduce a second medium, with index n_2 , forming a planar interface transverse to the optical axis at $z = z_o$. To describe reflection at this interface we decompose the spectrum of plane waves in Eq. (1) into s -polarized and p -polarized field components. With the Fresnel reflection coefficients $r^{(p)}$ and $r^{(s)}$, the reflected field becomes

$$\begin{aligned} \mathbf{E}_{\text{ref}}(\mathbf{r}) = & \frac{-ifE_o \exp(-ik_1 f)}{2\pi k_1^2} \sqrt{\frac{n_o}{n_1}} \\ & \times \iint_{k_x, k_y} \exp\{i[k_x x + k_y y - k_{z_1}(z - 2z_o)]\} \\ & \times \begin{bmatrix} k_x^2 k_{z_1} r^{(p)} - k_y^2 k_1 r^{(s)} \\ k_x k_y (k_{z_1} r^{(p)} + k_1 r^{(s)}) \\ k_x (k_x^2 + k_y^2) r^{(p)} \end{bmatrix} \frac{\sqrt{k_1/k_{z_1}}}{k_x^2 + k_y^2} dk_x dk_y. \quad (3) \end{aligned}$$

A similar expression can be derived for the transmitted field by use of the Fresnel transmission coefficients.

Using Eqs. (2) and (3), we can derive the far fields of the reflected field. After refraction at reference sphere f the reflected field turns into a collimated beam, which can be expressed in cylindrical coordinates (ρ, ϕ, z) as

$$\begin{aligned} \mathbf{E}_{\text{ref}}^\infty = & -E_o \exp\{2ik_1[1 - (f/\rho)^2]^{1/2} z_o\} \{[\cos^2 \phi r_p(\rho) \\ & - \sin^2 \phi r_s(\rho)]\hat{x} + \frac{1}{2} \sin 2\phi [r_p(\rho) + r_s(\rho)]\hat{y}\}, \quad (4) \end{aligned}$$

where \hat{x} and \hat{y} denote the transverse unit vectors. For an incident field focused on a perfectly reflecting interface located at $z_o = 0$ the reflection coefficients are $r_p = 1$ and $r_s = -1$. In this case we simply obtain $\mathbf{E}_{\text{ref}}^\infty = -E_o \hat{x}$, which is, except for the minus, identical to the assumed input field. Equation (4) allows us to plot the field distribution in a cross-sectional plane through the collimated reflected beam. We see that the Fresnel reflection coefficients modify the polarization and amplitude profiles of the beam, and, more important, also its phase profile. For no defocus ($z_o = 0$) phase variations arise only at radial distances $\rho > \rho_c$ for which the Fresnel reflection coefficients become complex numbers. The critical distance

corresponds to $\rho_c = fn_1/n_2$ and is the radial distance associated with the critical angle of total internal reflection [$\theta_c = \arcsin(n_2/n_1)$]. Inasmuch as $\rho_c < f_1$ there are no aberrations if $n_2 > n_1$. With Eq. (4) we are able to design suitable phase plates to compensate for the aberrations introduced by the phase variations.

After being refracted at the second reference sphere f' , the field $\mathbf{E}_{\text{ref}}^\infty$ turns into the far field needed by Eqs. (1) and (2) for calculating the electric field \mathbf{E}_{ref} near the focus of the second lens. To solve the resultant integrals we express the wave numbers k_x, k_y , and k_{z_3} in spherical coordinates (r, θ', ϕ) . As indicated in Fig. 1, angles θ and θ' are related by $\sin \theta / \sin \theta' = f'/f$, which allows us to express angle θ' in terms of θ . For longitudinal wave number k_{z_3} we obtain

$$k_{z_3} = k_3 \left(1 - \frac{f^2}{f'^2} \sin^2 \theta\right)^{1/2} \approx k_3 - \frac{k_3}{2} \frac{f^2}{f'^2} \sin^2 \theta, \quad (5)$$

where we have required that the second focusing lens have a much larger focal length than the first lens, i.e., $f/f' \ll 1$. After expressing field point \mathbf{r} in image space in cylindrical coordinates (ρ, φ, z) and retaining only the lowest orders of f/f' , we can express the image field as

$$\begin{aligned} \mathbf{E}_{\text{ref}}(\rho, \varphi, z) = & E_o \frac{k_3 f^2}{2if'} \exp[-ik_3(z + f')] \\ & \times [(I_0 + I_2 \cos 2\varphi)\hat{x} - I_2 \sin 2\varphi \hat{y}] \sqrt{\frac{n_o}{n_3}}, \quad (6) \end{aligned}$$

with

$$\begin{aligned} I_0(\rho, z) = & \int_0^{\theta_{\max}} \cos \theta \sin \theta [r_p(\theta) - r_s(\theta)] \\ & \times J_0(k_3 \rho \sin \theta f/f') \\ & \times \exp[(i/2)k_3 z (f/f')^2 \sin^2 \theta] \\ & + 2ik_1 z_o \cos \theta d\theta, \quad (7) \end{aligned}$$

$$\begin{aligned} I_2(\rho, z) = & \int_0^{\theta_{\max}} \cos \theta \sin \theta [r_p(\theta) + r_s(\theta)] \\ & \times J_2(k_3 \rho \sin \theta f/f') \\ & \times \exp[(i/2)k_3 z (f/f')^2 \sin^2 \theta] \\ & + 2ik_1 z_o \cos \theta d\theta. \quad (8) \end{aligned}$$

Here we have expressed the Fresnel reflection coefficients in terms of θ by using $k_{z_1} = k_1 \cos \theta$ and $k_{z_2} = k_2 [1 - (n_1/n_2) \sin^2 \theta]^{1/2}$. θ_{\max} is defined through $\text{NA} = n_1 \sin \theta_{\max}$, and the magnification of the system is $M = f'n_1/(fn_3)$. For numerical integration it is convenient to subdivide the integration range because the integrands in Eqs. (7) and (8) have discontinuities at the critical angle.

To discuss the field distributions in the image plane we choose $n_1 = 1.518$, $n_3 = n_o = 1$, and

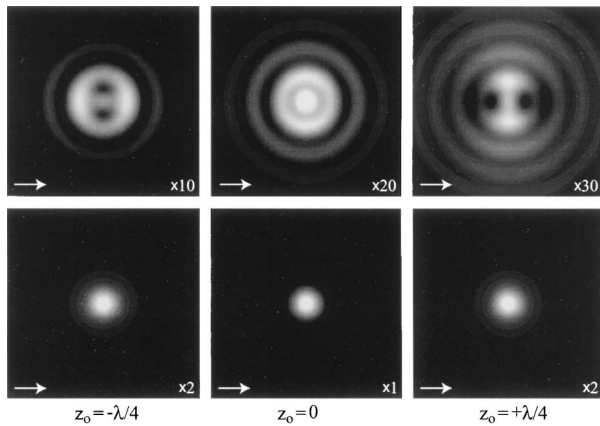


Fig. 2. Reflected images of a diffraction-limited focused spot. The spot is moved in steps of $\lambda/4$ across the interface. z_0 is positive (negative) when the focus is below (above) the interface. Upper row, glass–air interface ($n_2 = 1$); lower row, glass–metal interface ($\epsilon_2 \rightarrow -\infty$). The arrow indicates the direction of polarization of the incoming beam. Image size, $4.75M\lambda$.

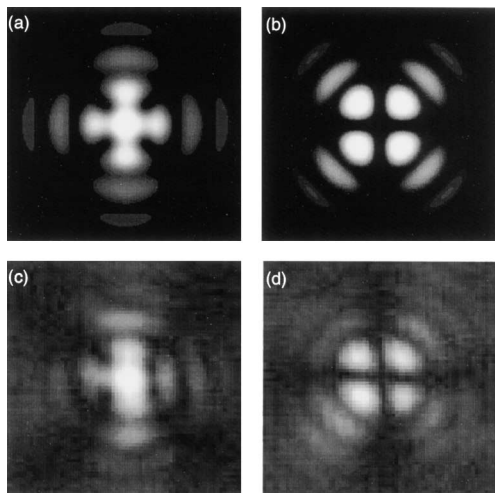


Fig. 3. Decomposition of the in-focus reflected image (upper center image of Fig. 2) into two orthogonal polarizations: (a), (c) polarization in the direction of the incident polarization (\hat{x}); (b), (d) polarization perpendicular to the incident polarization (\hat{y}). (a), (b) Calculated patterns, (c), (d) experimental patterns. Image size, $4.75M\lambda$.

$NA = 1.4$ ($\theta_{\max} = 67.26^\circ$). The images in the lower row of Fig. 2 depict the electric field intensity $|\mathbf{E}_{\text{ref}}|^2$ as a function of slight defocus for an ideally reflecting interface. The spot shape and size are not significantly affected by the defocus. However, as shown in the upper row of Fig. 2, the situation is quite different if the medium beyond the interface is a dielectric with an index of refraction $n_2 < n_1$. In this case the reflected spot changes greatly as a function of defocus and the spot shape deviates considerably from a Gaussian spot. The overall size of the spot is increased, and the polarization is not preserved (I_0 and I_2 are of comparable magnitude). The patterns displayed in Fig. 2 can be verified in the laboratory. However, some care has to

be applied when one is using dichroic beam splitters because they have slightly different characteristics for s - and p -polarized light. Using a polarizer in the reflected beam path allows one to examine the two polarizations separately, as shown in Fig. 3. Notice that the focus coincides with the interface when the center intensity of the reflected pattern $[I_0(\rho, z)]$ is maximized.

The origin of the observed aberrations lies in the nature of TIR. All plane-wave components with angles of incidence in the range $[0 \dots \theta_c]$, where θ_c is the critical angle of TIR (41.2°), have real reflection coefficients. Consequently there are no phase shifts between incident and reflected waves. However, plane-wave components in the range $[\theta_c \dots \theta_{\max}]$ undergo TIR at the interface, and the reflection coefficients become complex numbers. These complex reflection coefficients impose a phase shift between incident and reflected waves that can be viewed as an additional path difference between incident and reflected waves similar to the Goos–Hänchen shift. This phase shift displaces the apparent reflection point beyond the interface, thereby creating a second, virtual, focus.¹ We thus find the important result that the reflected light associated with the angular range $[0 \dots \theta_c]$ originates from the real focal point on the interface, whereas the light associated with $[\theta_c \dots \theta_{\max}]$ originates from a virtual origin located above the interface.

The observation of the aberrations in the focal point's reflected image has important consequences for reflection-type confocal microscopy and data sampling. In these techniques the reflected beam is focused onto a pinhole in the image plane. Because of the aberrations of the reflected spot, most of the reflected light is blocked by the pinhole, and this affects the sensitivity. However, it has been pointed out that this effect can dramatically increase the contrast between metallic and dielectric sample features.¹

This research was supported by Forschungsverbund Optoelektronik (FOROPTO) and National Science Foundation grant DMR-0078939. We thank M. Beversluis for recording the experimental images. The authors' e-mail addresses, in order, are novotny@optics.rochester.edu, robert.grober@yale.edu, and khaled.karrai@physik.uni-muenchen.de.

References

1. K. Karrai, X. Lorenz, and L. Novotny, *Appl. Phys. Lett.* **77**, 3459 (2000).
2. H. Maeckler and G. Lehmann, *Ann. Phys. (Leipzig)* **10**, 115, 153 (1952).
3. G. Lehmann and H. Maeckler, *Ann. Phys. (Leipzig)* **10**, 161 (1952).
4. T. D. Milster, J. S. Jo, and K. Hirota, *Appl. Opt.* **38**, 5046 (1999).
5. B. Hecht, B. Sick, and L. Novotny, *Phys. Rev. Lett.* **85**, 4482 (2000).
6. L. Mandel and E. Wolf, *Optical Coherence and Quantum Optics* (Cambridge U. Press, New York, 1995).
7. B. Richards and E. Wolf, *Proc. R. Soc. London Ser. A* **253**, 358 (1959).